



LAWRENCE
LIVERMORE
NATIONAL
LABORATORY

UCRL-TR-202117

CT Scans of NASA BSTRA Balls 5f5, f2, f3, sr2c, nb2a and hb2b

*Roger Perry, Randall Thompson,
Jeffery Gross, and Daniel Schneberk*

February 2, 2004

This document was prepared as an account of work sponsored by an agency of the United States Government. Neither the United States Government nor the University of California nor any of their employees, makes any warranty, express or implied, or assumes any legal liability or responsibility for the accuracy, completeness, or usefulness of any information, apparatus, product, or process disclosed, or represents that its use would not infringe privately owned rights. Reference herein to any specific commercial product, process, or service by trade name, trademark, manufacturer, or otherwise, does not necessarily constitute or imply its endorsement, recommendation, or favoring by the United States Government or the University of California. The views and opinions of authors expressed herein do not necessarily state or reflect those of the United States Government or the University of California, and shall not be used for advertising or product endorsement purposes.

Ct Scans of NASA BSTRA Balls 5f5, f2, f3, f4, sr2c, hb2a, hb2b

Roger Perry, Randall Thompson, Jeffery Gross and Daniel Schneberk

Introduction

At the request of Jose Hernandez we performed some feasibility DR/CT scanning of BSTRA Balls of different sizes. To this point we have scanned all the specimens on a single system, HECAT. This particular system employs a 9 meV LINAC as the x-ray source and a THALES 12 x 16 inch 14-bit Amorphous Silicon panel as the detector. In this report we describe the system, detail some of its properties, describe the scans performed and present the data.

Figure 1 contains a couple of images of the system as fielded in the 9 MeV bay. The LINAC is in the right portion of the picture. The black panels in the blue frame constitute the High Energy collimator developed specifically for High Energy DR/CT scanning (known here as Stonehenge II). The holes in the collimator panels are beveled to match the distribution of the x-rays from the LINAC, and are sized to just subtend the active area of the THALES Amorphous Silicon panel (see Figure 2). Consequently the source to detector distance is restricted to a few positions. Nominally our source to detector distance is 6 meters.

The part manipulator, part holder fixturing consists of a translate-rotate assembly on a NEWPORT air bearing table. The stages are NEWPORT RV160PP for rotation and NEWPORT IMS400CC for translation (see Figure 3). Both are interfaced through an ESP7000 controller, which is connected to our data acquisition computer over USB. The detector holder also resides on this table and includes pitch, roll and yaw adjustments for aligning the panel to the plane of the rotational table and the x-ray beam.

The relatively large source to detector distance and LINAC properties (1 mm spot size) conspire to recommend rotation-only scanning. We use a VARIAN LINATRON 3000 with the small spot retrofit implemented. We have measured the source spot size at about 1 mm. Pixel size on the THALES panel is 0.127 um. Consequently we are in a low-cone angle scanning regime which enables rotation-only 3D CT scanning of objects and assemblies with little “cone-angle” error.

Scan Parameters

All the scans were performed with the Stonehenge II collimator. Consequently the source to detector distance is about 6 meters (5775 mm). The object is approximately 20 inches from the detector (520 mm), putting the source to object distance at 5255 mm. With this geometry, the maximum cone angle is 2 degrees. For the objects we are scanning the cone angle ranges from 0.5 to 0.75 degrees. We are running the Am-Si panel in an un-binned format, 0.127 mm at the detector, and with this magnification, puts the voxel size for the reconstructed cubes of data at 0.116 mm. We have measured the spatial resolution of this data at approximately 210 um, using the ASTM PSF estimation

method on a tantulum cylinder containing holes. As corroboration of spatial resolution down to this scale, the cylinder contained some 250 um holes which could be seen in different slice planes of the 3D volume. The usual caveats for spatial resolution apply. It is possible to see high-contrast features which are smaller than 200 um. However, low contrast features will just be imaged at this spatial scale. All scans acquired involved 720 views acquired over 360 degrees, or 180 degrees, when the cone-angle was below 0.7 degrees.

Acquired Scan Data

3D CT Data was acquired on 9 NASA BSTRA Balls: 5f5, f2, f3, f4, sr2c, hb2a, and hb2b. Digital radiographs were reconstructed into 3D volumes using LLNL CT Preprocessing and reconstruction software. Each 3D volume resulted in a 3-4 GB volume of data. This data is now residing on a single FireWire Drive and will be shipped to NASA, as well as the software necessary to read and evaluate the images.

From discussions with NASA staff two analysis tasks were performed on this data. First the entire volumes were inspected for defects, holes or voids in the material. Secondly, we inspected the volumes for sub-surface defects. Inspection of the entire 3D volumes indicated no internal voids greater than 500 um. Further, we observed no indications of deep cracks or large changes in density.

Sub-surface layers were inspected with a “shell-extraction” technique. With this operation, we find the outer boundary of the BSTRA Ball using an intensity threshold, then using those boundary coordinates, we shrink or expand that shape, and extract a “shell” of pixels centered on that shrunk or expanded boundary. The 2D image producing this operation resembles a “mercator” plot, a common way to show the map of the earth on single 2D map. In an effort to see all the defects, our “mercator” plots overlap the circumference (390 degrees) of the shell at the user-selected depth. The features at the far end of the mercator map are duplicated, but we don’t miss any features which might be compromised by a 360 degree unwrapping. The extractions are guided by the position of the “outside boundary” estimated by the software (there are two choices, fit a circle, or shrink-wrap to an outside boundary). Consequently, small mismatches at the surface can lead to artifacts in the shell extraction image. Sometimes this results in a vertical band, extending pole to pole, getting larger at the waist than at the poles. This type of artifact can also arise from “ring artifacts” in the CT scans. Sequences of shell extraction images have been produced for all of the Balls scanned.

For all the specimens, we saw the least indications of issues with balls 5f5, f2, f4 and sr2c. Figures 4-7 contain shell extraction images of balls 5f5, f2, f4 and sr2c. Our scan of Ball f3 contained what appeared to be small sub-surface indications of lower porosity. Figure 8 contains a shell extraction image with suspect locations identified on the image. Scans of hb2a, and hb2b showed indications of some sub-surface etching of some kind, which appears to be machine made. The indications of lack of mass in hb2a and hb2b appear to be in straight lines in various positions. Figures 9-10 contain the shell extraction images of hb2a and hb2b, with the suspect positions highlighted. Notice the presence of the “vertical” features in some of the images in the figures. At this point we

consider these features artifacts of our shell extraction technique and in some cases indicate small but persistent “ring” artifacts in our CT reconstructed data.

In conclusion, our scans of balls 5f5, f2, f4, and sr2c showed little indication of any anomalies in the ball material. Scans of ball f3 indicated possible sub-surface defects we expect to be small porosity. Scans of balls hb2a and hb2b showing indications of etching close to the surface of the balls.



Figure 1 – Picture of HECAT components – LINAC & Stonehenge II Collimator.

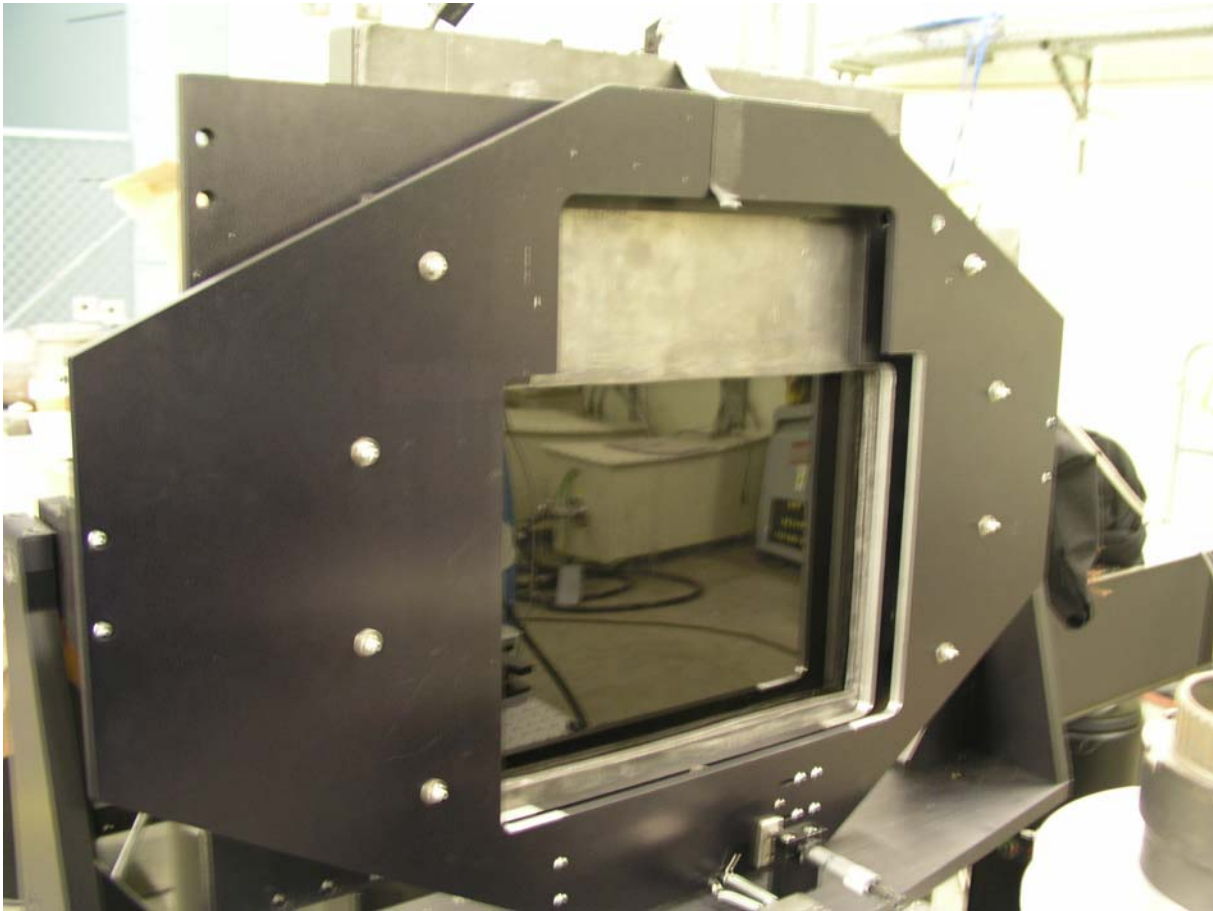


Figure 2 – Digital Photo of 12 x 16 inch THALES 14-bit Amorphous Silicon panel in holder showing active area of detector.

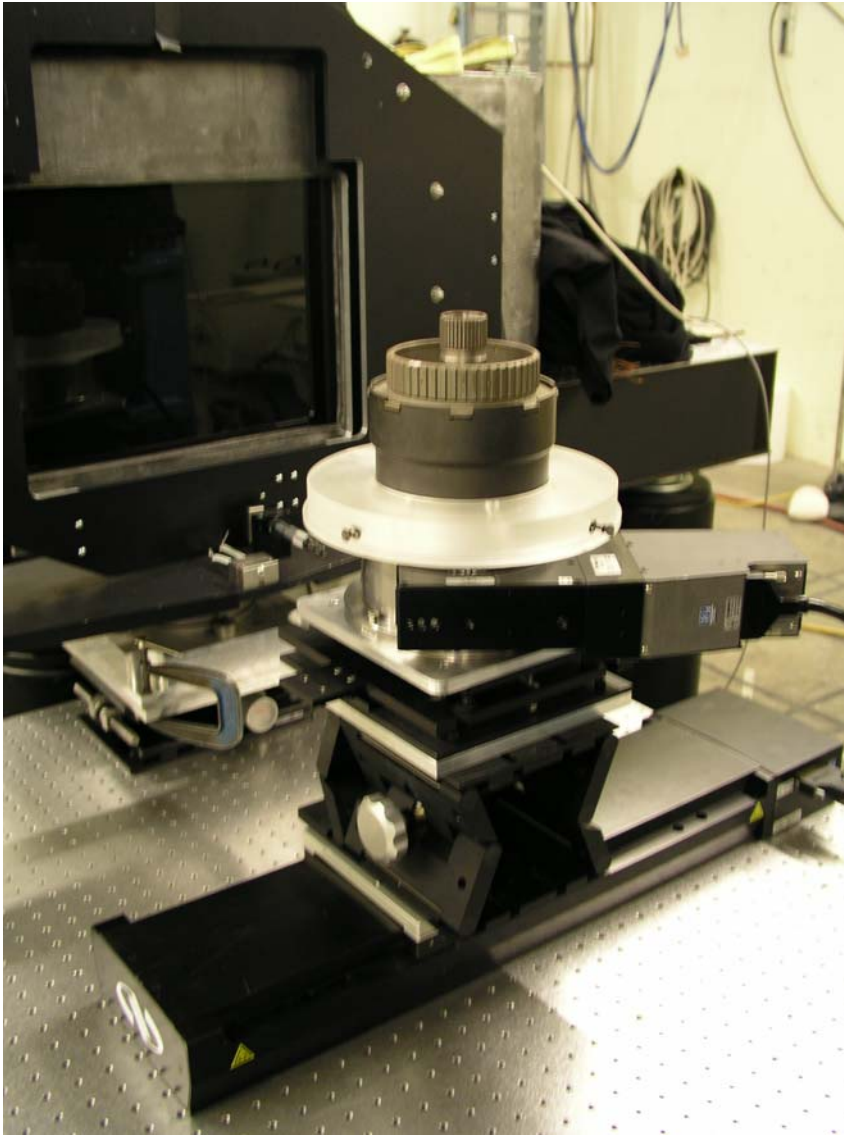


Figure 3 – Illustration of Object positioning system, with Industrial object loaded on rotary stage

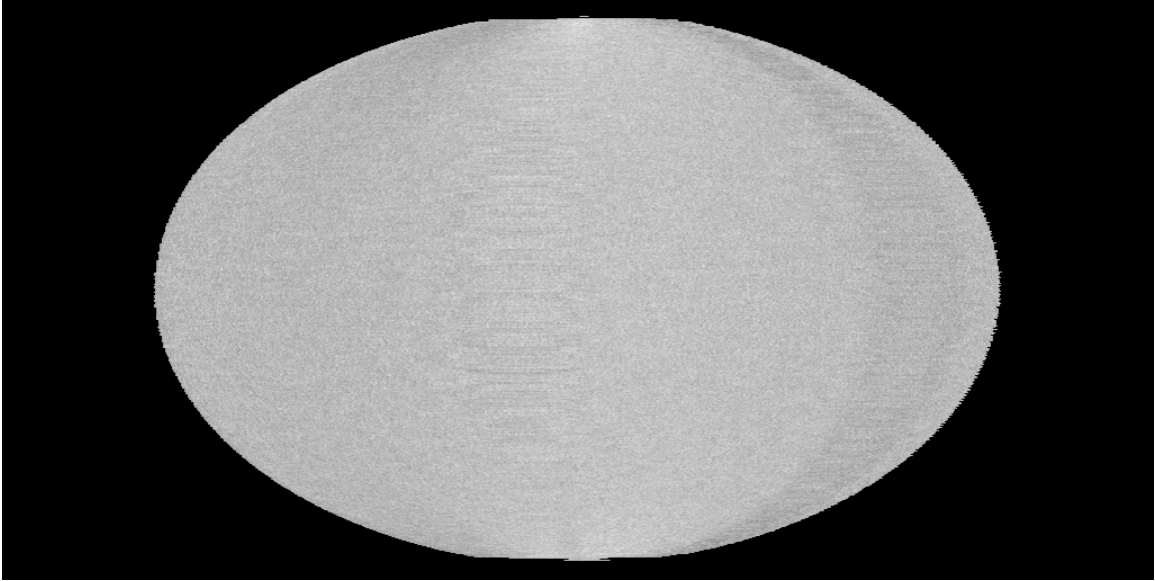


Figure 4 – Shell Extraction from Nasa BSTRA Ball - 5f5

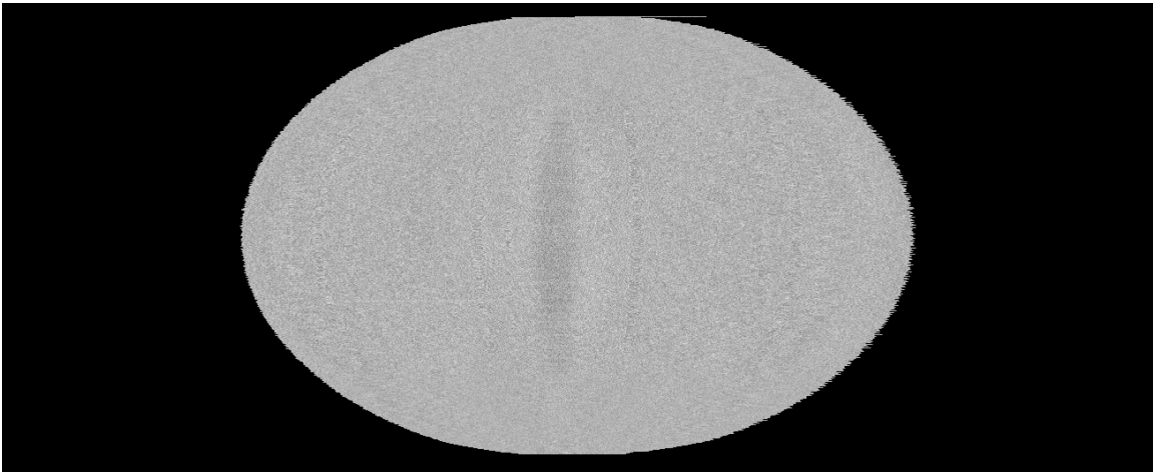


Figure 5 – Shell Extraction from Nasa BSTRA Ball – f2

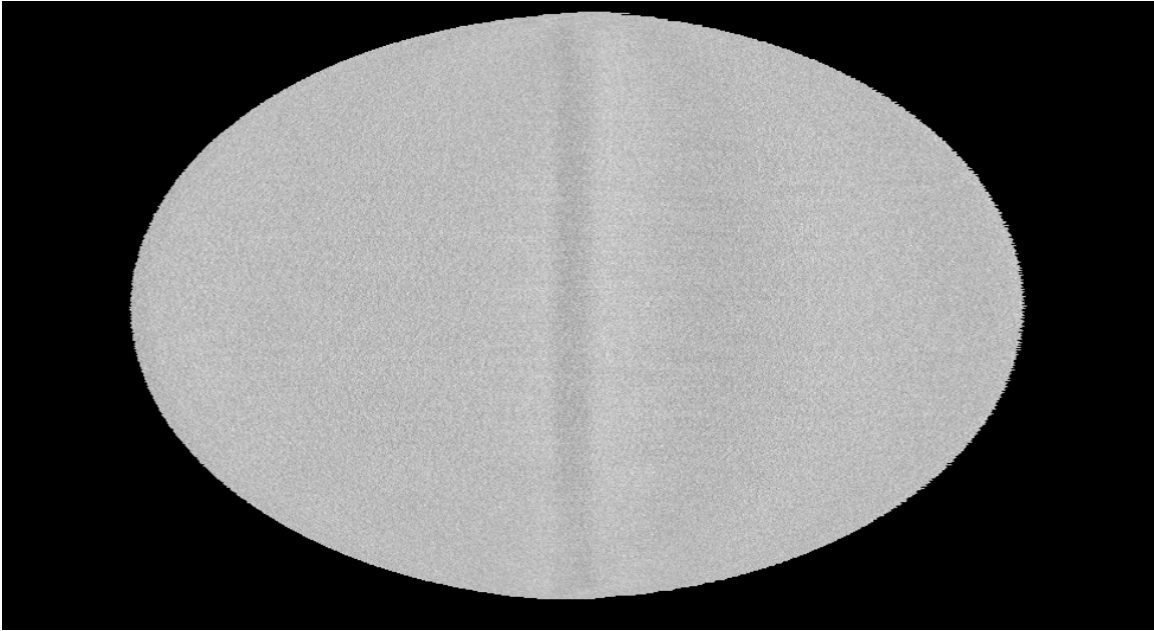


Figure 6 – Shell Extraction from Nasa BSTRA Ball – f4



Figure 7 – Shell Extraction from Nasa BSTRA Ball – sr2c

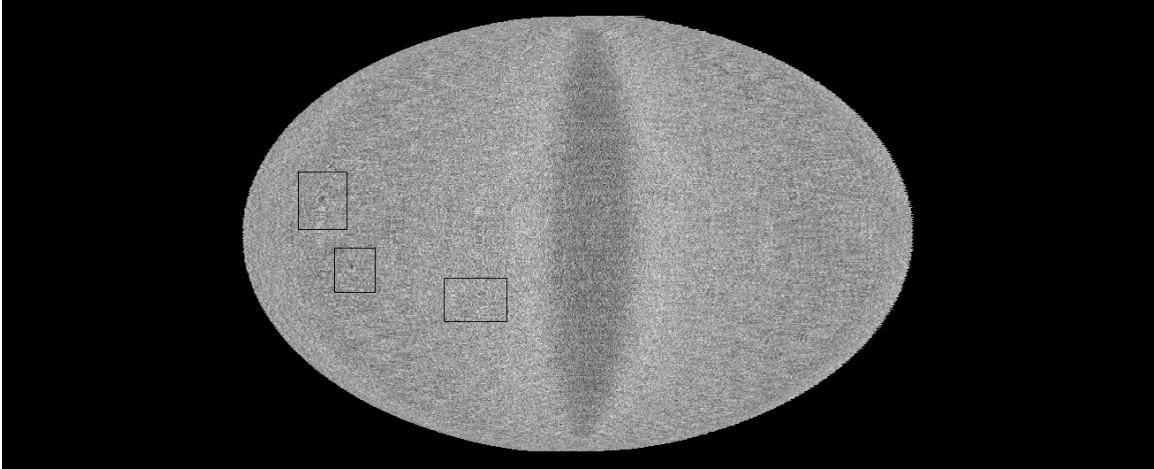


Figure 8 – Shell Extraction from NASA BSTRA Ball f3

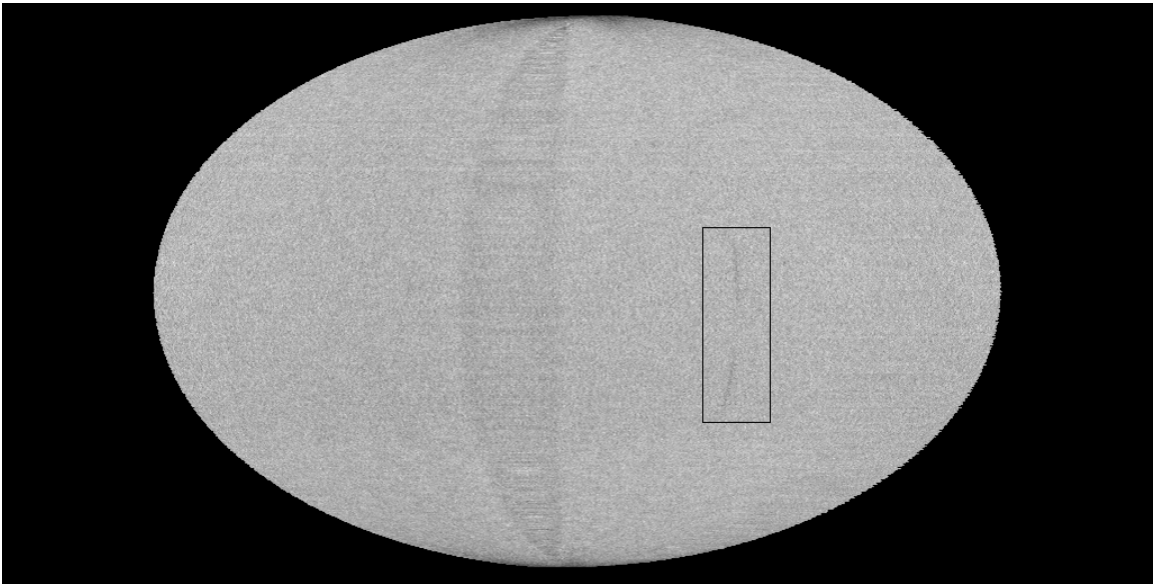


Figure 9 – Shell Extraction from Nasa BSTRA Ball – hb2a

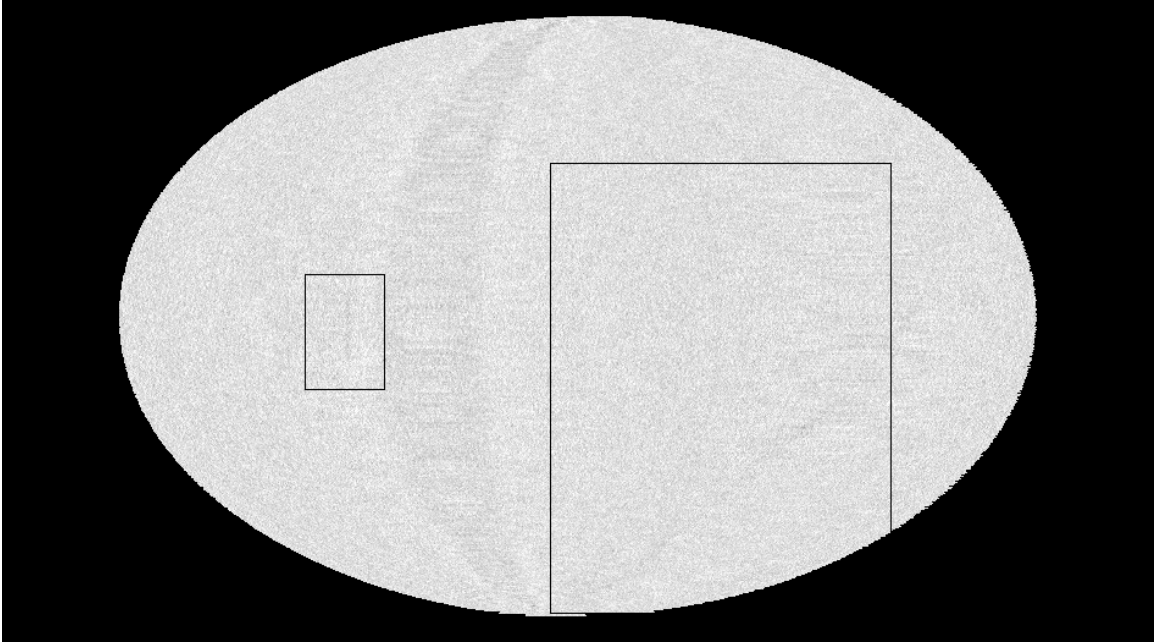


Figure 10 – Shell Extraction from Nasa BSTRA Ball – hb2b

This work was performed under the auspices of the U.S. Department of Energy by University of California, Lawrence Livermore National Laboratory under Contract W-7405-Eng-48.